DEPUNEREA ȘI CARACTERIZAREA FILMELOR SUBȚIRI PE BAZĂ DE WO_3 NANOSTRUCTURAT CA ELEMENTE SENZORIALE PENTRU DETECȚIA H_2S

DEPOSITION AND CHARACTERIZATION OF THIN FILMS BASED ON NANOSTRUCTURED WO_3 AS SENSORIAL ELEMENTS FOR DETECTION OF H_2S

A. SOBEȚKII[1±], M.T. OLARU[1±], U. CINDEMIR[2b], L. ÖSTERLUND[2b], A. STĂNOIU[3c], C.E. SIMION[3c], S.E. BEJAN[1*], R.E. IRIMESCU[1*]

[1]National Research & Development Institute for Non-ferrous and Rare Metals, High PT Met and Laboratory of Advanced and Nanostructured Materials, Biruinței, 102, Pantelimon, Ilfov, 077145, România

[2]Uppsala University, Department of Engineering Sciences, The Ångström Laboratory, SE-751 21 Uppsala, PO Box 534, SWEDEN

[3]National Institute of Materials Physics, Atomiștilor 405A, Măgurele, 077125, România .

±These authors have equally contributed to the paper

Thin nanostructured films are the state-of-the-art materials for detection of very low limits of toxic gases. The work presents a comparison between the properties of WO_3 thin films obtained by two different deposition techniques: Advanced Gas Deposition (AGD) and DC Reactive Sputtering. Films have been characterized by XRD, SEM and XPS. WO_3-based sensors have selective sensitivity in H_2S detection at operating temperature of 200°C and relative humidity specific to field applications. The potential interferences with CO_2, SO_2 and NH_3 are negligible, highlighting the application potential of WO_3.

Filmele subțiri nanostructurate sunt materiale de ultimă generație pentru detectarea concentrației foarte scăzute a gazelor toxice. Lucrarea prezintă o comparație între proprietățile filmelor subțiri de WO_3 obținute prin două tehnici diferite de depunere: Depunere avansată de gaze (AGD) și DC Reactive Sputtering. Filmele subțiri au fost caracterizate prin XRD, SEM și XPS. Senzorii pe bază de WO_3 prezintă sensibilitate selectivă în detecția H_2S la temperatura de operare de 200°C și umiditate relativă specific aplicațiilor din teren. Potențialele interferențe cu CO_2, SO_2 și NH_3 sunt neglijabile, evidențiind potențialul aplicativ al WO_3.

Keywords: *Gas sensing, Tungsten trioxide, Advanced Gas Deposition, DC Reactive Sputtering*

1. Introduction

In the last decade, there has been an increase in industrialization and automation which have led to the emission of toxic gases such as CO, H_2, NH_3, NO_X and SO_2 compounds which causes serious impact on the environment and also on human health [1-2]. Therefore, gas detection/monitoring is essential for industrial process control, vehicle emission control, environmental monitoring as well as public and home security. Most of the studies are focused on detecting CO, CO_2, O_2, SO_2, O_3, H_2, Ar, N_2, NH_3, VOCs, LPG, etc. because of their toxicity [3-6].

Sensors based on nanostructures play a significant role in the detection and monitoring of these toxic gases because of their high sensitivity, relatively low operating temperatures and a rapid response to the detected gas. Various materials such as metals, polymers, carbon-based materials and metal oxide semiconductors materials, etc. are widely used as sensing materials for sensors. Amongst all these materials, metal oxide semiconductors (MOS) such as zinc oxide (ZnO), titanium dioxide (TiO_2), tin oxide (SnO_2), tungsten oxide (WO_3), vanadium pentoxide (V_2O_5), and iron oxide (Fe_2O_3), cerium dioxide (CeO_2), nickel oxide (NiO) etc. are used as sensor materials because of their high response, excellent selectivity, simple working principles, and good portability [7-12]. The major reason for their potential is the high active surface-to-volume ratio, which could increase the rates of the surface reactions by increasing the number of adsorption centers on the surface of the sensor layer [13]. Compared with other oxide materials, WO_3 based sensors show remarkable performance because of their sensitivity in the detection of specific target gases such as O_2, NO_2, NH_3, and H_2S owing to their operability at elevated temperatures [14]. WO_3 has a variety of oxidation states, electronic structure and microstructure morphology, so obtaining it has a rich physical and chemical performance advantages, and it is widely used in sensor parts [15-19]. This material is non-stoichiometric. The crystal structure of WO_3 is very complex, available in different phases (i.e. cubic, hexagonal, monoclinic and orthorhombic). It is an n-type semiconductor material, having large band gap

* Autor corespondent/*Corresponding author*,
E-mail: sbejan@imnr.ro, ririmescu@imnr.ro

(2.6–3.25 eV), however monoclinic (P21/n) are more studied for gas sensing. Its lattice parameter is a = 7.30 Å, b = 7.53 Å and c = 7.69 Å [4]. Searching appropriate techniques for fabricating the nanostructured coatings is one of the current research goals.

Different deposition techniques have been used by researchers for the preparation of WO_3 thin films, such as, spray pyrolysis, chemical precipitation, RF and DC magnetron sputtering, chemical vapor deposition, sol-gel methods, pulsed laser deposition (PLD), etc. [20-25].

However, some of these methods have certain limitations such as: high thermal budget, complicated processing technique, use of catalyst, long processing time, high cost, adaptability for mass production, unwanted byproducts, not being environment-friendly [26].

The aim of the present paper is to compare the properties of WO_3 thin films obtained by two different deposition techniques: Advanced gas deposition (AGD) and DC Reactive Sputtering.

2. Experimental work

2.1. Materials

Two types of substrates were used initially for the thin film deposition to establish the optimal conditions. From tungsten pellets, purity 99,9% (Plasmaterials Inc., USA), WO_3 was deposited on glass microscope slides (Menzel Gläser, ThermoScientific) and silicon wafers (1 cm^2). DropSens Interdigitated Gold Electrodes IDEAU 200 (bands/gaps dimension 200µm, ceramic substrate dimensions: L 22.8 mm x W 7.6 mm x H 1 mm) were used as a substrate, at the end.

2.2. Sample preparation

a) Advanced Gas Deposition method

Nanocrystalline-nanoporous WO_3 thin-film samples were prepared by heating W pellets (purity 99.95%), placed in a carbon crucible, via an RF coil. The evaporated species were oxidized in a laminar gas flow comprising 0.1 l/min of oxygen (purity 99.998%) and 20 l/min of helium (purity 99.997%). The oxidized W nanoparticles thus formed were transported through the transfer pipe into the deposition chamber, where WO_3 deposits where formed on substrates attached to a programmable X–Y-moving platform. Helium was chosen as carrier gas since it is known to yield especially small particles.

b) DC Reactive Sputtering method

Nanocrystalline-nanoporous WO_3 thin-film samples were prepared by using a 2-inch tungsten sputtering target (purity 99.95%), commercially purchased from plasmaterials.com. The vacuum chamber was initially evacuated at a base pressure of $2.66 \cdot 10^{-4}$ Pa to remove all gas impurities and then backfilled by introducing a laminar gas flow comprising 50ml/min of argon (purity 99.99%) and 8 ml/min of oxygen (purity 99.998%). Plasma was ignited at a partial pressure of 4 Pa and by applying a DC power of 240 W at the cathode (the W target). The ionized argon gas atoms are driven to the substrate which is the anode attracting gas ions, electrons and the vaporized target coating atoms which oxidize during transfer and condense to form the WO_3 thin film coating.

Preliminary tests were done on glass microscope slides and silicon wafers, and the optimum deposition parameter results were selected, after a close analysis of all the process conditions, so that the specific thickness of commercial sensors to be obtained. Later on, they were used on Interdigitated Gold Electrodes to obtain the sensors.

For Advanced Gas Deposition (AGD) method, the varying process parameters were power and speed. The power is the parameter that has a major influence on the thickness and the porosity (in terms of adherence) of the film. After a close analysis of the data set obtained after 5 attempts, the optimal values to obtain the proper thickness of the film, are 1.3 KW for power and 1000 st/s for speed.

For DC Reactive Sputtering (DC) method, the W target was of approximately 5 cm and the varying process parameter was the time - influencing the film thickness. After 2 attempts could be established that the optimum time was of 45 minutes and the power of 227 W.

The two samples analyzed below were denoted S1 (for AGD) and S2 (for DC sputtering).

2.3. Characterization

The X-ray diffraction (XRD) for thin films data were taken using a Siemens 5000 diffractometer with CuKα1 radiation, with a 2θ range from 20° to 80° and the incident angle was kept at 1°. Film morphologies were determined by scanning electron microscopy (SEM) for silicon substrate on which WO_3 was deposited, using a Zeiss LEO 1550 FEG instrument with in-lens detector. The film thickness was measured via VeecoDektak 150 surface profilometry instrument. The X-ray photoelectron spectroscopy (XPS) measurements were recorded within a PHI Quantum 2000 Scanning ESCA Microprobe with a monochromatic Al Kα1 radiation X-ray source, having a beam diameter of 200 µm. Survey scans were measured with a pass energy of 93.9 eV and resolution of 0.4 eV where high resolution scans were measured with a pass energy of 23.50 eV and 0.025 eV resolution. Energy range of the survey scans were 1100-0 eV. To control charging of the samples, a neutralizer filament is used in all measurements. Adventitious carbon's 1s peak at 248.8 eV is used to calibrate spectra in order to correct peak shifts due to charging.

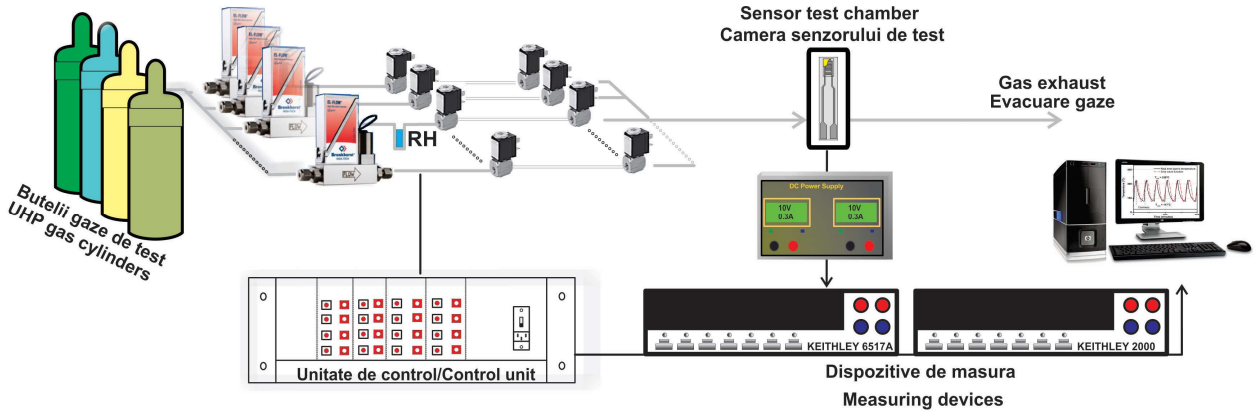

Fig. 1 - Experimental set-up used for evaluation of the sensing performances of WO_3-DC and WO_3-AGD based gas sensors.
Instalația experimentală utilizată pentru evaluarea performanțelor de detectare a senzorilor de gaz WO_3-DC și WO_3-AGD.

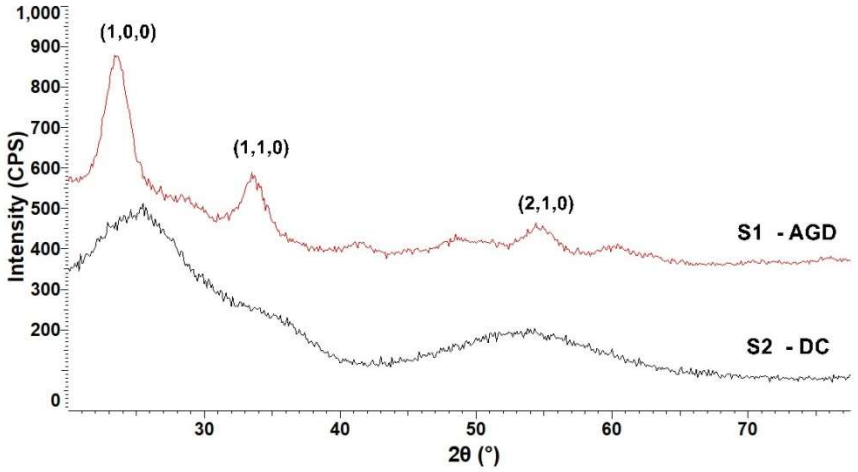

Fig. 2 - XRD pattern of S1 sample (WO_3 deposited by AGD) and S2 sample (WO_3 deposited by DC reactive sputtering).
Graficul DRX al probei S1 (WO_3 depus prin AGD) și al probei S2 (WO_3 depus prin DC reactive sputtering).

The sensing properties have been evaluated by a fully computer-controlled gas mixing system (GMS) equipped with high grade certified test gases. The GSM unit consists in eleven gas channels each of them driven by Bronkhorst mass flow controllers and two solenoid electrovalves (Figure1).

The electrical resistance measurements of the WO_3 gas sensor structures have been done using a Keithley 6517 A electrometer and Keithely 2000 A multimeter.

3. Results and discussions

3.1. X-ray Diffraction (XRD)

Figure 2 presents the XRD spectra of the WO_3 thin films deposited by AGD and DC reactive sputtering. The qualitative analysis of the spectra shows the formation of cubic WO_3 phase.

Even though the layer of WO_3 was deposited onto a glass substrate and analyzed with X-ray diffraction (XRD), the pattern presented an amorphous type style, making the calculus of the crystallites size doubtful, since the representative peaks of WO_3 are unclear. The peaks tend to present a big broad size, indicating small crystallites size of around 28.9 nm. The size of the crystals was computed using Scherrer formula applied on integral breadth. The cell parameter presents a value between 3.71 nm and 3.77 nm.

The XRD spectra belonging to sample S2 deposited by sputtering do not show very clear peaks, indicating an amorphous structure. However, sample S1 have tetragonal ∝-phase structure with some high intensity peaks. The first broad peaks contain both (001) at 22.9° and (200) at 24.1°, due to small crystallite size.

When comparing the results from X-ray diffraction patterns, the AGD technique yields more crystalline samples compared to the DC sputtering technique.

3.2. Scanning electron microscopy (SEM)

A comparison between the results obtained through AGD and DC reactive Sputtering is presented in Figure 3.

The SEM analysis showed that the WO_3 films deposited by AGD have a more porous structure than the films achieved by sputtering. In terms of sensing properties this characteristic is

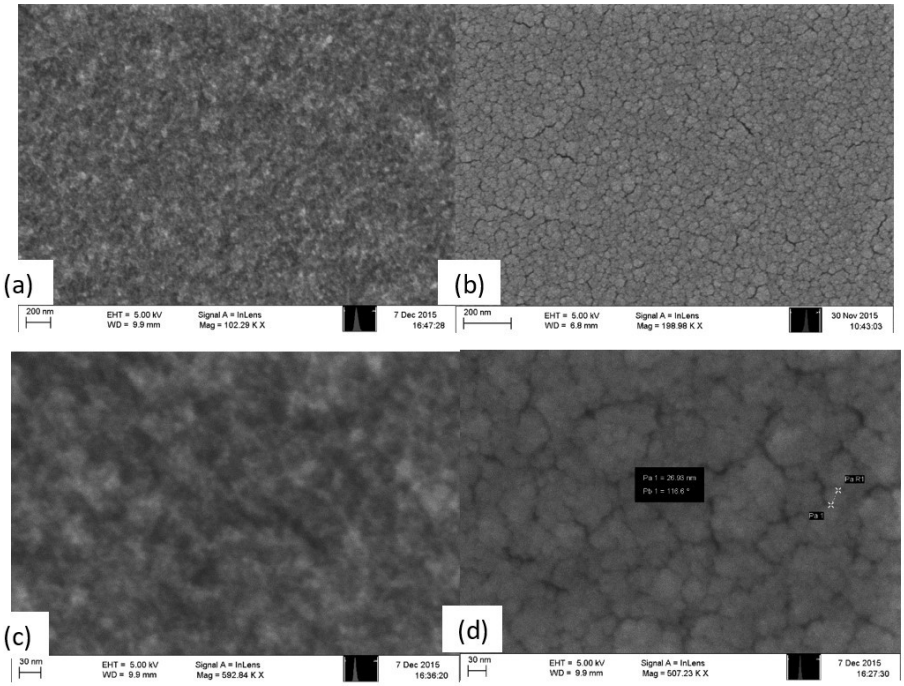

Fig. 3 - SEM micrographs of a) and c) sample S1 (WO_3 deposited by AGD); b) and d) sample S2 (WO_3 deposited by DC Reactive Sputtering). */ Micrografii SEM ale probei S1 (WO_3 depus prin AGD) - (a) și (c); și a probei S2 (WO_3 depus prin DC Reactive Sputtering) – (b) și (d).*

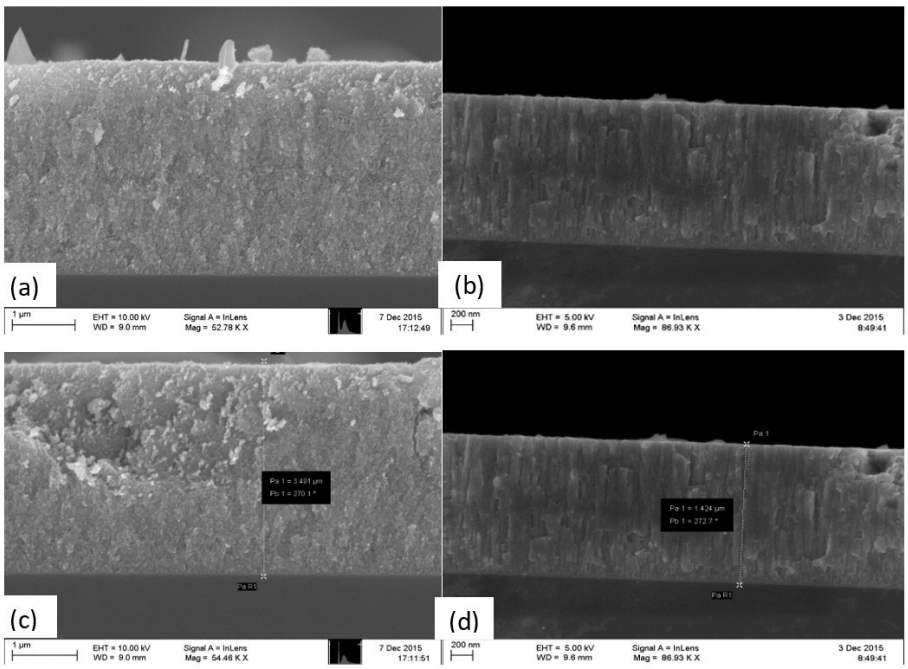

Fig. 4 - Cross section of SEM micrographs: a) sample S1 (WO_3 deposited by AGD); b) sample S2 (WO_3 deposited by DC Reactive Sputtering). / *Secțiunea transversală a micrografiilor SEM: proba S1 (WO_3 depus prin AGD) - (a); și proba S2 (WO_3 depus prin DC Reactive Sputtering) – (b).*

important since the porosity tends to favor the passing of current more freely, thus improving the conductivity of the sensor.

Typical columnar growth can be seen for the sputtered film with a particle size of 27nm. The film thickness for sample S1 determined by cross section in SEM is of 3400 nm, while for sample S2 is of 1400 nm (Figure 4).

3.3. X-ray photoelectron spectroscopy (XPS)

The surveys scans in the XPS spectra were used to determine the elemental concentrations. Carbon can be noticed in the samples, due to o possible contamination from the graphite crucible. The name of each peak, their relative sensitivity factors, area and corresponding atomic percentages were shown in Table 1. Survey scans

Table 1

XPS survey scan results of the samples. / *Rezultatele scanării probelor prin XPS*

Sample / *Proba*	Name / *Nume*	R.S.F.	Area / *Suprafata*	% Conc.
Sample S1 / *Proba S1*	C 1s	1	118.96	27.3
	O 1s	2.93	582.45	45.61
	W 4f	9.8	1156.95	27.09
Sample S2 / *Proba S2*	C 1s	1	143.16	31.45
	O 1s	2.93	567.84	42.58
	W 4f	9.8	1158.35	25.97

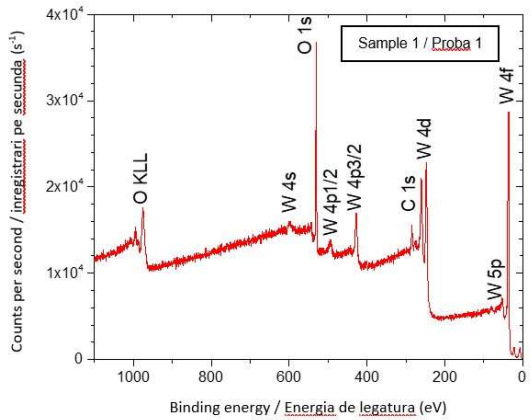

Fig. 5 - XPS survey scan of sample S1 (WO_3 deposited by AGD) with corresponding regions. / *Rezultatele scanării prin XPS a probei S1 (WO_3 depus prin AGD) cu regiunile corespunzătoare.*

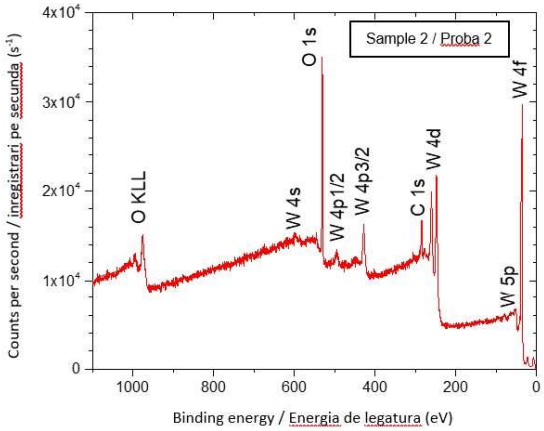

Fig. 6 - XPS survey scan of sample S2 (WO_3 deposited by DC reactive sputtering) with corresponding regions. / *Rezultatele scanării prin XPS a probei S2 (WO_3 depus prin DC reactive sputtering) cu regiunile corespunzătoare.*

were shown with their regions corresponding to core levels at their binding energies in Figure 5 and Figure 6.

In Figure 7, the W $4f_{5/2}$ and W $4f_{7/2}$ peak doublet has been analyzed for chemical identification. The small peak around 42 eV is a characteristic loss feature for WO_3. The area ratios of 4f5/2 and 4f7/2 peaks are 3:4. With the constraint of ratios, after fitting the peaks to Gaussian-Lorentzian peaks, it turns out that there is a tiny contribution from WO_2 components as well. The amount of WO_2 to WO_3 ratios are 3% and 6%, in sample 2 and sample 1, respectively.

3.4. Sensing properties

Figure 8 illustrates the sensing properties of the WO_3 structures to different test gases (H_2S, CO_2, SO_2 and NH_3) with respect to the operating temperature. The sensor signals were calculated according to the following relation:

$$S_{red} = {R_{air}}/{R_{gas}},$$

where R_{air} is the electrical resistance under reference atmosphere (synthetic air 5.0 with 50% relative humidity as in the field conditions) and R_{gas} is the electrical resistance under specific detection limit for each test gas.

The highest response (S>400) was obtained with WO_3-DC sensor for 20 ppm H_2S, when operated at 200°C (Figure 8 a). Potential interferences with CO_2 (S=4), SO_2 (S=2) and NH_3 (S=1.5) are negligible (Figure 8 b-d). Even for the WO_3-AGD sensor which is less sensitive to H_2S (S>100), the selectivity is pronounced. Obviously, the sensing response has a strong correlation with the thickness of the sensitive layer, respectively with the deposition technique.

The sensitivity of the WO_3 sensors upon H_2S exposure can be explained by the physical-chemical mechanism (Figure 9) based on H_2S interaction with the pre-adsorbed oxygen (O_2^-) which results in an increase in the number of free carriers in the conduction band.

Such description is in good agreement with specific literature for this domain [28-29].

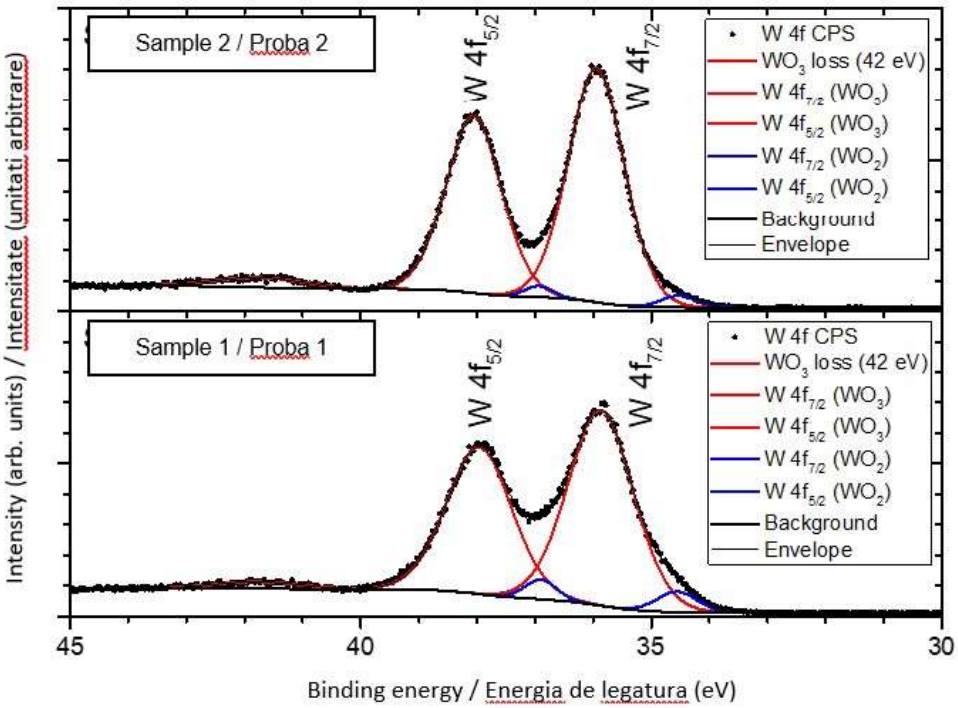

Fig. 7 - XPS W4f core-level spectra of samples S1 (WO_3 deposited by AGD) and S2 (WO_3 deposited by DC reactive sputtering) are shown with corresponding fits. */ Spectrele XPS W4f ale probelor S1 (WO_3 depus prin AGD) și S2 (WO_3 depus prin DC reactive sputtering) sunt prezentate cu fitările corespunzătoare.*

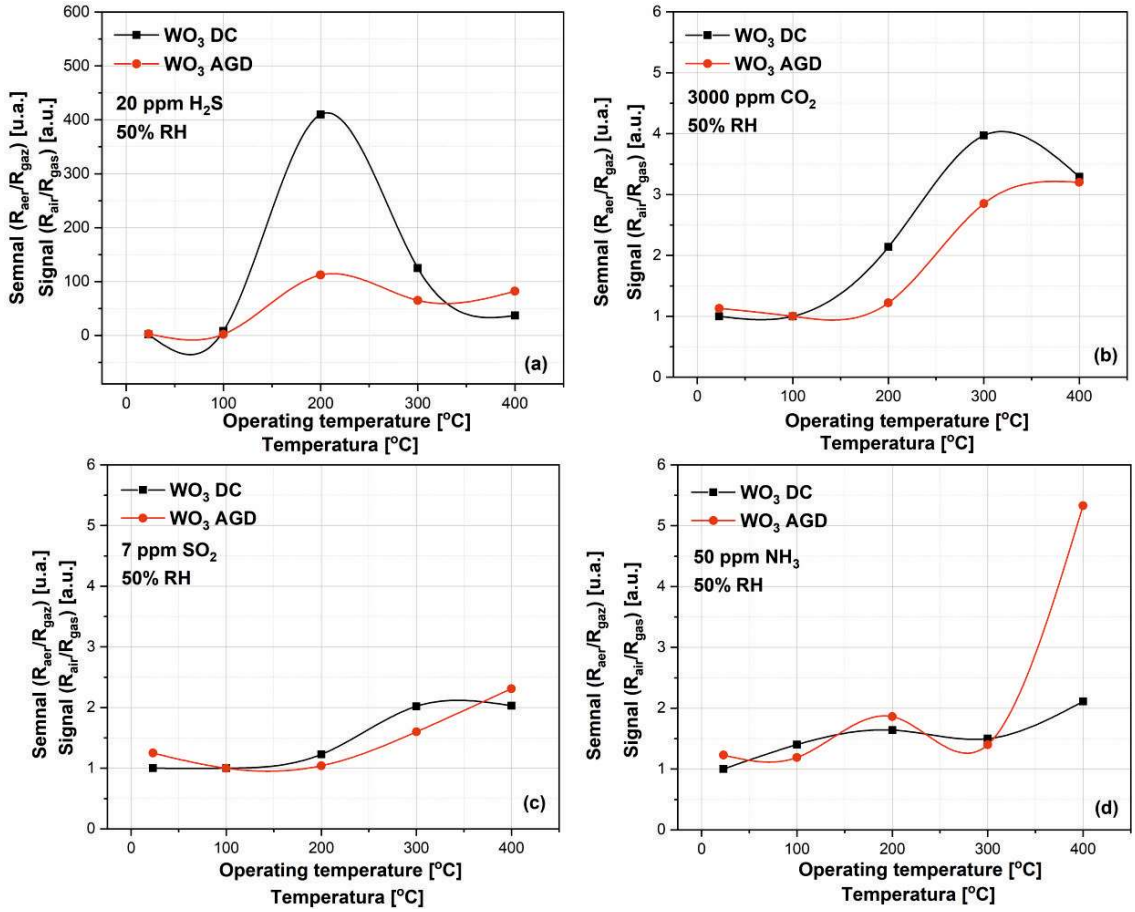

Fig. 8 - Sensing properties modulated by the operating temperature. */ Proprietăți de detectare modulate de temperatura de funcționare.*

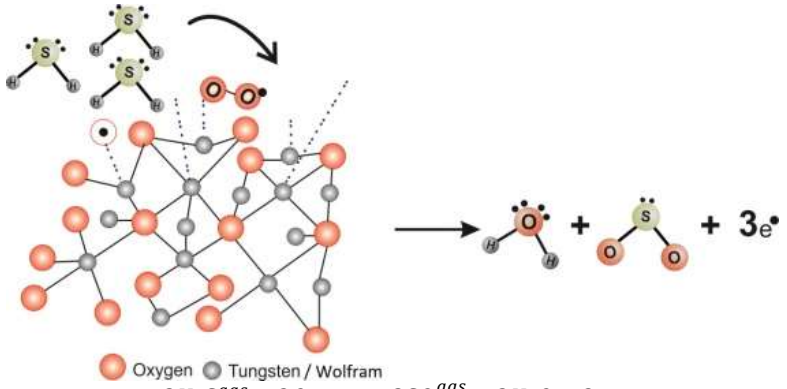

Fig. 9. - The physical-chemical mechanism of WO_3 sensitivity to H_2S. / *Mecanismul fizico-chimic de sensibilitate a WO_3 la H_2S.*

4. Conclusions

The present paper considered different deposition techniques to obtain WO_3 thin films.

A comparison between the sputtering and advanced gas deposition was performed, through a detailed structural and morphological characterization of WO_3 thin films. It has been observed that the films produced via AGD are more porous, thus making the AGD technique more accurate in obtaining a better film on the sensor, which offers a better conductivity.

The WO_3 - DC and WO_3 - AGD sensors have been investigated towards different test gases (NH_3, CO_2, SO_2 and H_2S) under real operating conditions. The highlighted selective sensitivity to H_2S suggests the applicative potential of WO_3 thin layers.

Acknowledgements:

This work was supported by a grant of the Romanian National Authority for Scientific Research, CNDI–UEFISCDI, project number 198/2012- SENSGAS UEFISCDI, the European Union's Horizon 2020 Research and Innovation program under grant agreement 645758 RISE-TROPSENSE 2015-2019, the European Research Council under the European Community's Seventh Framework Program (FP7/2007–2013)/ERC, Grant Agreement No. 267234 ("GRINDOOR") and Program Nucleu, contract no. 6N/2019 (Project code PN 19 19 04 01/2019), a grant from the Ministry of Research and Innovation.

The authors thank to PhD D.V. Dragut, for XRD analysis, to PhD O.G. Florea for gas property measurements and to PhD R.M. Piticescu Who was in charge for TROPSENSE Project and supervising training at Uppsala University.

REFERENCES

[1]. S.A. Beknalkar, V.L. Patil, N.S. Harale, M.P. Suryawanshi, A.P. Patil, V.B. Patil, J.H. Kim, P.S. Patil - 2-D to 3-D Conversion of WO_3 Nanostructures Using Structure Directing Agent for Enhanced NO_2 Gas Sensing Performance, Sensors and Actuators: A. Physical, 2020.

[2]. N. Yamazoe - New approaches for improving semiconductor gas sensors, J. Sensors Actuators B. Chem., 1991, **5** (1–4), 7–19.

[3]. World Health organization Report - www.who.int&assets&pdf file&A.

[4]. S. Mahajana, S. Jagtap - Metal-oxide semiconductors for carbon monoxide (CO) gas sensing: A review, Applied Materials Today, 2020.

[5]. G. Eranna, B.C. Joshi, D.P. Runthala, R.P. Gupta - Oxide materials for development of integrated gas sensors - a comprehensive review, Crit. Rev. Solid State 2010, (29), 111–188.

[6]. Q. Du, L. Wang, J. Yang, J. Liu, Y. Yuan, M. Wang, B. Liu, X. Zhang, Y. Ren, H. Zhao, H. Yang - Sensors and Actuators B: Chemical, 2018, (273), 1786-1793.

[7]. P.S. Chauhan, S. Bhattacharya - Hydrogen gas sensing methods, materials, and approach to achieve parts per billion level detection: A review, International Journal of Hydrogen Energy, 2019, **44**(47), 26076-26099.

[8]. E. Comini, G. Faglia, G. Sberveglieri - Electrical-based gas sensing, Solid State Gas Sensing, Springer, New York, 2009.

[9]. K. Arshak, I. Gaidan - Development of a novel gas sensor based on oxide thick films, Sci. Eng. B, 2005, (118), 44–49.

[10]. H. Khan, et al. - Quasi physisorptive two-dimensional tungsten oxide nanosheets with extraordinary sensitivity and selectivity to NO_2, Nanoscale 2017, **9**, 19162.

[11]. M. Alsaifa, S. Balendhrana, M.R. Field, K. Athamb, W. Wlodarskia, J.Z. Ou, K.K. Zadeh - Two dimensional α-MoO3 nanoflakes obtained using solvent-assisted grinding and sonication method: application for H2 gas sensing, Sensors and Actuators, B, 2014, (192), 196–204.

[12]. J.Z. Ou, W. Ge, B. Carey, T. Daeneke, A. Rotbart, W. Shan, Y. Wang, Z. Fu, A.F. Chrimes, W. Wlodarski, S.P. Russo, Y.X. Li, K. Kalantar-zadeh - Physisorption based charge transfer in two-dimensional SnS2 for selective and reversible NO2 gas sensing, ACS Nano 9, 2015, 10313–10323.

[13]. G. Atanasovaa, A. Og. Dikovskab, T. Dilovaa, B. Georgievac, G.V. Avdeevd, P. Stefanova, N.N. Nedyalkovb - Metal-oxide nanostructures produced by PLD in open air for gas sensor applications, Applied Surface Science, 2019, (420), 861-869.

[14]. B. Nam, T.K. Ko, S.K. Hyun, C. Lee - Sensitivities of a 6:4 (by molar ratio) ZnO/WO_3 composite nanoparticle sensor to reducing and oxidizing gases, Applied Surface Science, 2020, (504), 144104.

[15]. G. Jeevitha, D. Mangalaraj - Ammonia sensing at ambient temperature using tungsten oxide (WO_3) nanoparticles, Materials Today: Proceedings, 2019, (18), 1602–1609.

[16]. C. Zhai, M. Zhu, L. Jiang, T. Yang, Q. Zhao, Y. Luo, M. Zhang - Fast triethylamine gas sensing response properties of nanosheets assembled WO_3 hollow microspheres, Appl. Surf. Sci., 2019, (463), 1078–1084, https://doi.org/10.1016/j. apsusc.2018.09.049.

[17]. A.C. Anithaa, K. Asokan, C. Sekarv - Low energy nitrogen ion beam implanted tungsten trioxide thin films modified indium tin oxide electrode-based acetylcholine sensor, J. Taiwan Inst Chem E., 2018, (84), 11–18, https://doi.org/ 10.1016/j.jtice.2018.01.001.

[18]. Y. Xiong, Z. Zhu, T. Guo, H. Li, Q. Xue - Synthesis of nanowire bundle-like WO3- W18O49 heterostructures for highly sensitive NH3 sensor application, J. Hazard Mater., 2018, (353), 290–299, https://doi.org/10.1016/j.jhazmat.2018.04.020.

[19]. C. Xiao, L. Zhang, H. Hao, W. Wang - High selective oxidation of benzyl alcohol to benzylaldehyde and benzoic acid with surface oxygen vacancies on W18O49/holey ultrathin g-C3N4 nanosheets, Acs Sustain Chem Eng, 2019, (7), 7268–7276, https://doi.org/10.1021/acssuschemeng.9b00299.

[20]. Y. Fan, X. Xi, Y. Liu, Z. Nie, Q. Zhang, L. Zhao - Growth mechanism of immobilized WO3 nanostructures in different solvents and their visible-light photocatalytic performance, Journal of Physics and Chemistry of Solids, 2020, (140), 109380.

[21]. C. Castillo, G. Cabello, B. Chornik, Y. Huentupil, G.E. Buono-Core - Characterization of photochemically grown Pd loaded WO_3 thin films and its evaluation as ammonia gas sensor, Journal of Alloys and Compounds, 2020, (825), 154166.

[22]. M.B. Johansson, B. Zietz, G.A. Niklasson, L. Osterlund, Optical properties of € nanocrystalline WO_3 and WO_3-x thin films prepared by DC magnetron sputtering, J. Appl. Phys., 2014, (115), 213510.

.

[23]. X. Leng, J. Pereiro, J. Strle, A.T. Bollinger, I. Bozovic - Epitaxial growth of high quality WO_3 thin films, Apl. Mater., 2015, (3), 096102.

[24]. H. Simchi, B.E. McCandless, T. Meng, W.N. Shafarman - Structural, optical, and surface properties of WO_3 thin films for solar cells, J. Alloys Compd., 2014, (617), 609.

[25]. T. Caruso, M. Castriota, A. Policicchio, A. Fasanella, M.P. De Santo, F. Ciuchi, G. Desiderio, S. La Rosa, P. Rudolf, R.G. Agostino, E. Cazzanelli - Thermally induced evolution of sol-gel grown WO_3 films on ITO/glass substrates, Appl. Surf. Sci., 2014, (297), 195.

[26] A. Maity, S.B. Majumder - NO_2 sensing and selectivity characteristics of tungsten oxide thin films, Sensor. Actuator. B Chem., 2015, (206), 423.

[27] B. Beheraa, S. Chandrab - Synthesis of WO_3 nanorods by thermal oxidation technique for NO_2 gas sensing application, Materials Science in Semiconductor Processing, 2018, (86), 79-84.

[28] R. Ionescu, A. Hoel, C. G. Granqvist, E. Llobet, P. Heszler - Low-level detection of ethanol and H_2S with temperature-modulated WO_3 nanoparticle gas sensors, Sens. Actuators B., 2005, (104), 132-139.

[29]. A.D. Busuioc, R. Enuţă, Ş. Stoleriu, T. Vişan - SnO_2 based ceramics for gas sensors, Romanian Journal of Materials 2017, **47** (4), 419 – 424.

****